ELSEVIER

Journal of Chromatography B, 688 (1997) 281–289

JOURNAL OF CHROMATOGRAPHY B

Narrow-bore liquid chromatography–tandem mass spectrometry with simultaneous radioactivity monitoring for partially characterizing the biliary metabolites of an arginine fluoroalkyl ketone analog of D-MePhe-Pro-Arg, a potent thrombin inhibitor

Timothy G. Heath[a,*], Joseph P. Mooney[a], Robert Broersma[b]

[a]*Hoechst Marion Roussel, P.O. Box 9627, Kansas City, MO 64134-0627, USA*
[b]*Hoechst Marion Roussel, P.O. Box 156300, Cincinnati, OH 45215-6300, USA*

Received 1 May 1996; revised 24 June 1996; accepted 28 June 1996

Abstract

Characterizing components eluting from a HPLC column is enhanced when multiple detectors are incorporated in-line. The performance of a system consisting of a combination of two detectors – electrospray ionization mass spectrometry (and tandem mass spectrometry) and radioactivity monitoring, following gradient separation with a 250×2.1mm I.D. (Vydac Protein and Peptide C_{18}, 5 μm, 300 Å) column – is evaluated with respect to chromatographic integrity and detection. The HPLC effluent was split (8:1) and a post-column make-up solvent was added to flow directed towards the radioactivity detector containing a solid glass cell. Trifluoracetic acid (0.1%) was added to the make-up flow solvent to prevent silanol interactions from degrading the profile displayed in the ^{14}C trace. A ^{14}C chromatographic peak representing 550 dpm was detected with signal-to-noise ratio of 3. This system was used for rapidly characterizing the biliary metabolites of an arginine fluoroalkyl ketone analog of D-MePhe-Pro-Arg, a potent thrombin inhibitor currently being evaluated as a drug candidate. These metabolites are shown to comprise of mono- and dihydroxylated drug as well as a reduced ketone form of the drug. Combining the radioactivity monitor in-line with the mass spectrometer ensured that all of the major metabolites (as evident from the ^{14}C profile) were characterized by mass spectrometry.

Keywords: Arginine fluoroalkyl ketone; D-MePhe-Pro-Arg; Thrombin

1. Introduction

With the advent of atmospheric pressure ionization, coupling high-performance liquid chromatography (HPLC) with a mass spectrometer has become a relatively routine technique in a bioanalytical laboratory. For many detectors used with HPLC, the analysis of biological matrices typically requires sufficient sample processing to ensure that metabolites are discerned from endogenous components. A decrease in the chromatographic resolution may be tolerated with a mass spectrometer detector, however, due to the added dimension of mass resolution. Detection and structural characterization of drug metabolites by tandem mass spectrometry (MS–MS) [1–16], an approach pioneered by Yost et al. [1–3], may be accomplished following the direct analysis of a biological sample with minimal processing.

*Corresponding author.

PII S0378-4347(96)00299-X

There is a need to "locate" either temporally (chromatographically) or by m/z value, the metabolites present in the sample before one can characterize its structure. An initial analysis of a sample may rely on a strategy to merely screen for their presence. Tandem mass spectrometry offers screening approaches such as precursor ion scanning and/or constant neutral loss (CNL) scanning by relying on formation of diagnostic fragment ions following collision induced dissociation (CID). These screening approaches based on MS–MS have both strengths and weaknesses which have been highlighted by Naylor et al. [12]. Metabolites that undergo non-expected fragmentation pathways following CID or those which result from unusual biotransformations may not be detected. These limitations may preclude detection of major metabolites [9,12]. Overcoming these potential limitations requires alternative schemes, one of which is to use multiple HPLC detectors to simultaneously monitor analytes in metabolite screening. Radiolabeled drugs are used to make the metabolic profiling, isolation and identification easier. The on-line combination of tandem mass spectrometry and radioactivity monitoring (RAM) provides two selective and complementary detection modes which ensures detection of major metabolites.

While the utility of on-line detectors combined with mass spectrometry is widely recognized as a useful approach for characterizing drug metabolites, analytical HPLC columns (4.6 mm I.D.) are typically used [8]. The inherent sensitivity advantage offered by narrow-bore HPLC as a result of the lower flow-rate is desirable for electrospray ionization (ESI–MS) detection. However, the lower flow-rate used for narrow-bore columns can degrade the radiochomatographic peak shape as the volume of the flow cell is relatively large. Good peak shape may be maintained with smaller volume flow cells, yet this would reduce ^{14}C sensitivity. There are few literature reports describing narrow-bore HPLC–RAM–MS detection [17,18].

To provide another tool for our laboratory to rapidly screen and detect drug metabolites in biological matrices, we have interfaced narrow-bore HPLC with simultaneous RAM and ESI–MS detection. In our work, the HPLC effluent was split (8:1) with most of the flow directed towards the RAM detector equipped with a glass solid cell. To minimize the degradation of the radiochromatographic peak shape [19], however, a make-up flow was added to the effluent directed towards the radioactivity detector. The modifications required to accommodate simultaneous dual detection by RAM and ESI–MS following narrow-bore HPLC are described in this report. One intent of this report is to characterize the chromatographic efficiency and the limit of ^{14}C detection of this HPLC system. A second intent of this report is to demonstrate an initial application of this system for screening rat biliary metabolites of an arginine fluoroalkyl ketone analog of D-MePhe-Pro-Arg (I), a potent thrombin inhibitor whose structure is shown in Fig. 1. The major metabolites were detected and characterized by MS–MS as evidenced by the correlation of the radioactivity profile with the ion chromatograms generated by the mass spectrometer.

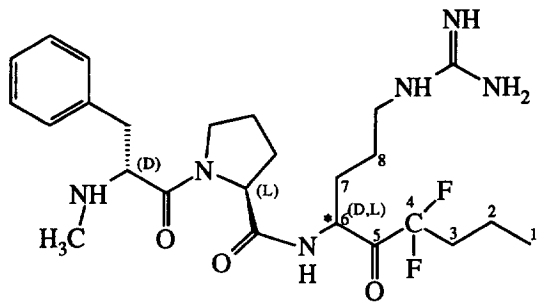

Fig. 1. Structure of compund I. The asterisk (*) indicates the site of the ^{14}C label.

2. Experimental

2.1. Materials

Radiolabeled (specific activity, 17.7 μCi/mg) and unlabeled I were obtained from Hoechst Marion Roussel Research Institute (Cincinnati, OH, USA). HPLC grade acetonitrile and trifluoroacetic acid were from the same source (Burdick and Jackson, Muskegon, MI, USA), while water was purified through a NANOpure II system (Barnstead, Dubuque, IA, USA).

2.2. Animals

Male Sprague–Dawley rats (225–350 g) were purchased from Harlan Sprague Dawley (Indianapolis, IN, USA). Rats were anesthetized with pentobarbital sodium (65 mg/kg, i.p.) and a jugular vein cannulated for drug administration. Biliary excretion was followed after intravenous injection of ^{14}C-labeled I (5 mg/kg) in rats. Bile was collected for a period of 45 min.

2.3. Instrumentation

Chromatographic separations were performed with a Michrom BioResources Ultrafast Microprotein Analyzer (Michrom BioResources, Pleasanton, CA, USA) HPLC system. The HPLC column was a Vydac Protein and Peptide C_{18}, 5 μm, 300 Å, 250×2.1 mm I.D (Phenomenex, Torrance, CA, USA). The column was maintained at 85°C. Following chromatographic separation, 0.128 mm I.D. PEEK tubing delivered the effluent to a PEEK tubing tee to split the flow, directing ~40 μl/min via fused-silica capillary tubing (FSC, 100 μm I.D./360 μm O.D.) to a Finnigan MAT TSQ 700 mass spectrometer equipped with an electrospray ionization source (Finnigan MAT, San Jose, CA, USA). The heated electrospray capillary was maintained at 250°C and the nose cone needle was at 3 kV. Low energy CID mass spectra were obtained using argon as the collision gas at 0.23 Pa, and a collision energy of 25–30 eV (E_{Lab}). The remainder of the effluent was delivered via a short piece of PEEK tubing (0.128 mm I.D.) to a second PEEK tee which served as a mixing chamber for post-column addition of 0.7 ml/min of a mixture of water–acetonitrile (50:50, v/v) with 0.1% TFA. This post column make up solvent was delivered by a Varian Model 2510 HPLC pump (Varian Analytical, Palo Alto, CA, USA). Following this second tee, the flow was directed to a β-RAM Model 2 flow-through monitor (IN/US Systems, Fairfield, NJ, USA) for radioactivity monitoring. A Cerium-activated scintillating solid lithium glass cell, with a volume of 400 μl was used in these studies. The total flow directed through this flow cell was ~960 μl/min. The analog output signal from the radioactivity monitor was imported into the data system of the Finnigan TSQ mass spectrometer allowing the the ^{14}C chromatographic profile to be viewed with Finnigan's ICIS software.

2.4. Chromatographic conditions

Mobile phase A consisted of water–acetonitrile (90:10, v/v) with 0.1% TFA, while B consisted of water–acetonitrile (10:90, v/v) with 0.1% TFA. The flow was maintained at 300 μl/min. A linear gradient from 90% A to 40% A in 22 min followed by a 3-min hold at 40% A was used to achieve chromatographic separation. The rat bile was passed through a disposable syringe filter and diluted 1:1 with mobile phase A prior to analysis. The injection volume was typically 30 μl.

3. Results and discussion

3.1. System characterization

Compound I contains three asymmetric centers. The configuration of two of the chiral centers is fixed while the third exists as a D/L pair. Hence, the compound exists as a mixture of two diastereomers. Epimerization occurs at C5 (note Fig. 1). A keto-hydrate equilibrium which degrades the chromatographic resolution, is established in the presence of water. Elevated temperature shifts the equilibrium in favor of the keto form which significantly improves the chromatographic peak shape. The two diastereomers may be readily resolved under reversed-phase conditions at low pH when the HPLC column is maintained at 85°C.

Radiolabeled I was used to determine the optimal chromatographic conditions for simultaneous ^{14}C and mass spectrometric detection. A flow-rate of 300 μl/min provided narrow chromatographic peaks for both detectors. The optimal flow-rate for the make-up solvent which mixed with the effluent directed towards the radioactivity detector was determined to be 0.7 ml/min (50:50, acetonitrile–water +0.1%TFA). Following the analysis of I, representative separations at these conditions as displayed by the reconstructed ion chromatogram (RIC) of MH^+ (m/z 509) and the radioactivity profile are shown in Figs. 2A and B. The peak-widths at base, w_b, for the RIC profile average 54 s, while the w_b for the peaks

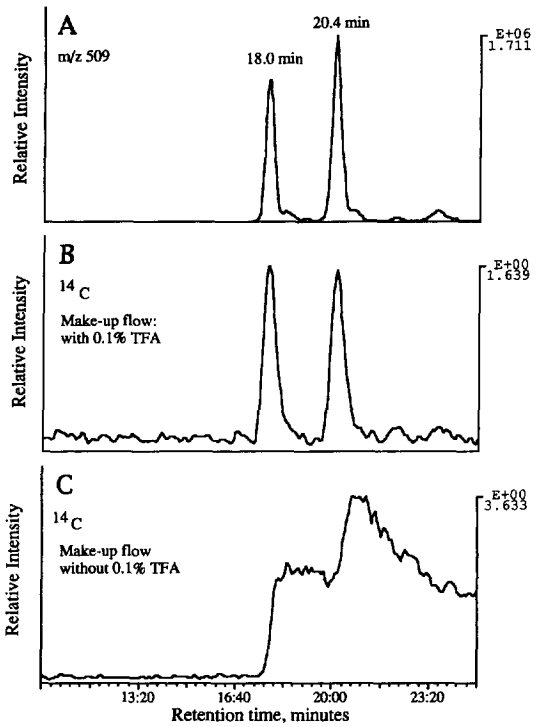

Fig. 2. The chromatographic profiles following the injection of I (~6000 dpm) onto the chromatographic system described in Section 2.3: (A) reconstructed ion current of MH^+ at m/z 509; (B) radioactivity (^{14}C) detector with make-up flow to the radioactivity monitor consisting of acetonitrile–water (50:50, v/v) with 0.1% TFA; (C) radioactivity (^{14}C) detector with make-up flow to the radioactivity monitor consisting of acetonitrile–water (50:50, v/v) without 0.1% TFA. The chromatograms displayed in (A) and (B) were acquired from the same analysis, while (C) was obtained in a separate analysis.

in the radioactivity trace (Fig. 2B) average 65 s. The two chromatographic profiles are nearly simultaneous with each other as the volume of the FSC tubing directed towards the mass spectrometer was only 2–3 μl thereby eliminating any lag time. Changes in the make-up flow-rate effect sensitivity for ^{14}C detection and the apparent (not actual) efficiency of the chromatographic separation as represented by the peak resolution depicted in the chromatographic trace [19]. To increase the residence time of the analyte within the solid glass cell, thereby increasing the response of the radioactivity monitor, the make-up flow-rate could be lowered. However, lowering the make-up flow-rate would increase the width of the chromatographic peak. During the course of this work, other compositions of make-up flow were investigated. Shown in Fig. 2C is the radioactivity chromatographic profile obtained with the make-up solvent consisting of acetonitrile–water (50:50, v/v) without 0.1% TFA. The chromatographic peaks as displayed in the RIC trace are virtually identical to those observed in Fig. 2A (data not shown); however, the chromatographic peaks observed in the radioactivity profile indicate severe degradation of the chromatographic separation. We propose that silanol effects are causing the poor peak shape [19]. Presumably, basic sites (Arg) on I interact with exposed silanols in the glass cell which are not protonated at more neutral pH conditions, thereby degrading the peak shape. Finally, Fig. 3 shows the detector profiles obtained following the injection of I with total radioactivity measured by

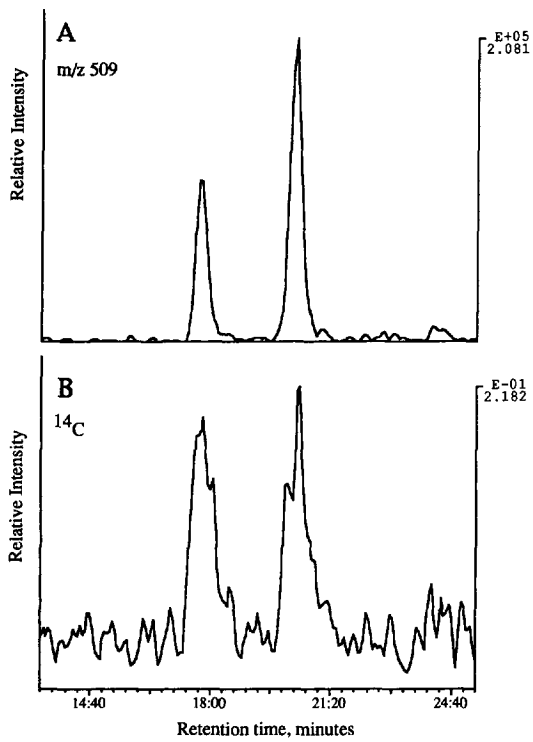

Fig. 3. The LC–MS/^{14}C chromatographic profiles obtained following the injection of 1100 dpm of compound I onto the chromatograph. Panel A represents the reconstructed ion profile of MH^+ at m/z 509 and panel B shows the ^{14}C trace.

off-line liquid scintillation counting, to be 1100 dpm, (~550 dpm per diastereomer). The ^{14}C signal depicted as a peak in the chromatogram (Fig. 3B) has a *S/N* of 3. This limit of detection is comparable to what is achieved in our laboratories with conventional analytical HPLC columns (4.6 mm I.D.) and a flow-rate of 1.0 ml/min with a 400-μl volume solid glass cell. By achieving comparable ^{14}C detection with a lower flow-rate, the sensitivity advantage is maintained for the concentration dependent electrospray ionization.

3.2. MS–MS of I

Because an initial application of this system involved the analysis of rat bile for rapid screening and characterization of metabolites of I, the fragmentation pattern of the protonated parent drug molecule was determined. The complete CID product ion mass spectrum of protonated I is shown in Fig. 4. The CID spectrum of each diastereomer appears identical. In addition, compound I was dissolved in deuterated methanol and infused directly into the electrospray ionization source of the mass spectrometer (data not shown). The mass spectrum indicated that 7 protons were exchanged with deuterium. The CID mass spectrum of the fully deuterated compound aided in assigning structures to fragment ions.

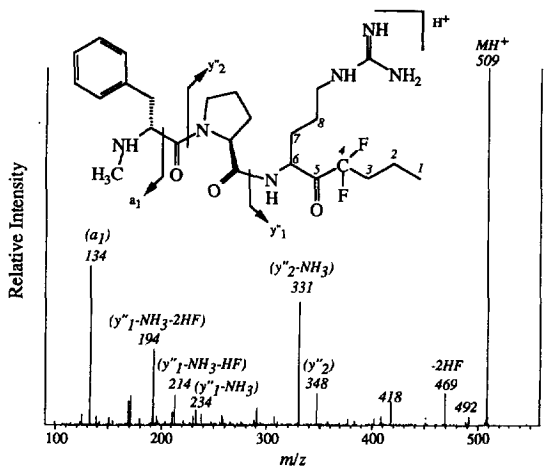

Fig. 4. The CID product ion mass spectrum of MH^+ of I at *m/z* 509. The CID spectrum was obtained at a collision energy of 25 eV (Lab), with argon in the second quadrupole at a pressure of 0.23 Pa. The product ion mass spectra of the two diastereomers of I are identical. See Refs. [20,21] for nomenclature of peptide fragmentation.

The major product ions following CID of MH^+ of I are indicated in Fig. 4. Facile cleavage of the peptide backbone to generate a_1 (*m/z* 134) occurs when MH^+ is subjected to CID. When compound I was infused in deuterated methanol and *m/z* 516 was subjected to CID, the a_1 ion was observed at *m/z* 135. Compound I also gave rise to prominent (y_2'') ions and (y_2''-NH_3) ions at *m/z* 348 and *m/z* 331 respectively. Loss of ammonia is a characteristic fragmentation pathway of peptide ions protonated at a basic arginine residue [22]. An additional product ion that appeared to be diagnostic for particular substructures of the molecule was observed with *m/z* 194. Further characterization of *m/z* 194 was obtained by increasing the capillary voltage, thereby offering a means for acquiring "pseudo" MS–MS–MS data. A precursor ion scan of *m/z* 194 was acquired at these conditions. These data suggest that *m/z* 194 represents the (y''_1-NH_3-2HF) species as parent ions of *m/z* 194 included *m/z* 251 (y''_1), *m/z* 234 (y''_1-NH_3) and *m/z* 214 (y''_1-NH_3-HF) all of which were detected as minor peaks in the CID mass spectrum of MH^+. Additional evidence for this ion assignment was obtained by examining the CID mass spectrum of an analog which differs from I in that the fluoroalkyl moiety is unsaturated at C1–C2. The ion designated (y''_1-NH_3-2HF) was detected with *m/z* 192. This fragment ion species is diagnostic for those metabolites where structural modifications are made to the C-terminal region of the molecule.

Ion structures were assigned to the more abundant fragment ions since some major CID fragmentation patterns were elucidated. Negative ion detection was investigated, yet the MS–MS data did not reveal additional structural information. Characterization of the CID mass spectrum of I was important so that any mass shifts in the fragment ions upon CID of protonated metabolites may be correlated to the appropriate substructure of the molecule. Such MS–MS data provides information regarding the sites of biotransformation, which in turn can impact structure-activity relationship studies and the design of new drug candidates.

3.3. Analysis of rat bile

The pharmacokinetic behavior of I after intravenous administration is characterized by a relatively short half-life of 16–37 min in rats and monkeys. One possible reason for this is rapid hepatic uptake of the compound and subsequent biliary excretion. Other thrombin inhibitors such as amidinophenylalanine amide derivatives, arginine amides, as well as the tripeptides derivatives share a common feature for an excretory route; they are eliminated via the bile to a significant degree [23–25]. Following i.v. administration of ^{14}C-labeled I in rats, 42% of the dose was excreted in the bile within 45 min and we sought to characterize the drug related components.

Concurrent radioactivity and mass spectrometry detection eliminates the need of tedious fraction collection for subsequent mass spectrometry analysis, following only RAM profiling. The location of drug related components via ^{14}C detection and mass spectrometric characterization is accomplished in the same chromatographic analysis. The utility of this chromatographic system was initially evaluated by the direct analysis of bile collected from rats dosed with compound I. Shown in Fig. 5 are representative chromatograms obtained over the course of these analyses. Fig. 5A is the radioactivity trace obtained concurrently with ESI–MS detection. Fig. 5B is the total ion current (TIC) trace for this same analysis. Essentially all of the radioactivity detected elutes in the region between the arrows as indicated in Fig. 5A. The mass spectral scans were summed over this region containing most of the radioactivity, and the mass spectrum is shown in Fig. 6A. Because only one level of mass selectivity is offered in this LC–MS analysis, the MH^+ of drug or metabolites which are representated by mass spectral peaks, are dispersed among all the peaks representing ionized endogenous components. The molecular weight information provided by the m/z values detected in these eluting components is "hidden" amongst the chemical noise. However, an additional level of mass selectivity is offered in the tandem mass spectrometry analysis of rat bile, and the mass spectrometry chromatographic profile following the precursor ion scan of m/z 134, is shown in Fig. 5C. When the ion current is summed to include the

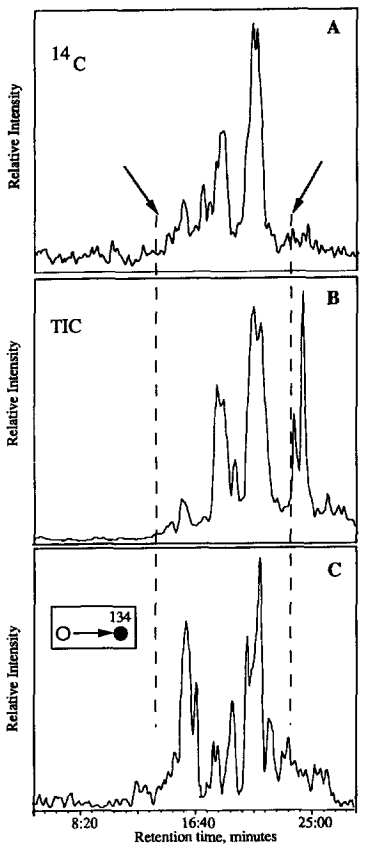

Fig. 5. Chromatographic profiles following the analysis of bile collected from a rat dosed with I: (A) ^{14}C profile; (B) TIC observed from the LC–MS aquisition; (C) TIC observed following a precursor ion scan of m/z 134. Chromatograms shown in (A) and (C) were obtained in the same analysis.

chromatographic region for which radioactivity is detected, the resulting precursor ion mass spectrum contains fewer mass spectral peaks as seen in Fig. 6B. The four prominent ions detected as peaks in this MS–MS analysis were at m/z 509, 511, 525 and 541. These analytes represent drug related components as they yielded the diagnostic fragment ion of m/z 134 upon CID and radioactivity was detected in the effluent. Based on the molecular mass information from the precursor ion scan analysis, we postulated that these ions represented the parent drug (m/z 509) as well as a reduced compound (m/z 511), and mono- and di-hydroxylated I (m/z 525, 541) as one or both diastereomeric forms. A complete CID product ion mass spectrum was acquired for each of

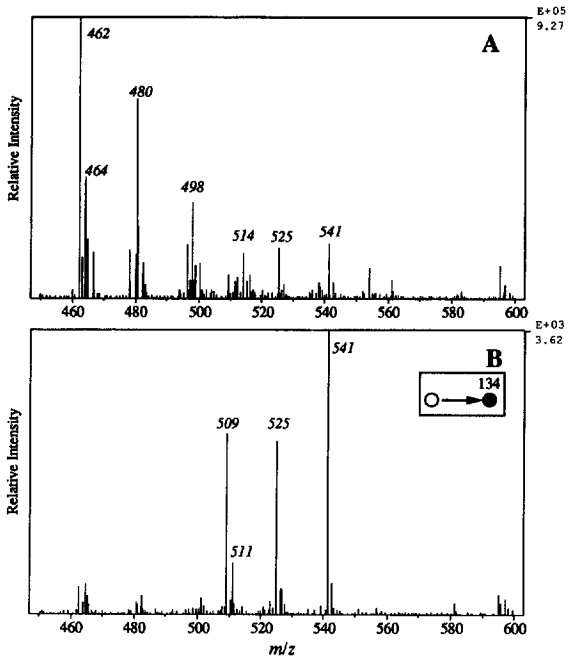

Fig. 6. Mass spectra obtained following the summation of ion current for which there was concurrent ^{14}C detection (as depicted in Figure 5). (A) LC–MS; (B) LC–MS–MS scanning for precursors of m/z 134.

these ions to further characterize the molecular structure.

The CID product ion mass spectra for the four ions with m/z 509, 511, 525 and 541 are shown in Fig. 7. The similarity of the CID product ion mass spectrum of m/z 509 with authentic I confirms the presence of parent drug in rat bile. The CID mass spectrum of m/z 511 indicated the y_2'' ion appears as a peak at m/z 350 along with the ion representing (y_2''-NH_3) at m/z 333. These data are consistent with a reduction of the Pro amide or Arg ketone moieties to a hemi aminal or hemi acetal functionalities. The absence of the (y''_1-NH_3-2HF) species in the CID of m/z 511 may imply reduction of the ketone functionality at C5. It wouldn't be expected that reduction at the Pro amide would prevent formation of (y''_1-NH_3-2HF) yet reduction at C5 may conceivably alter fragmentation at this region. The CID product ion mass spectra of both m/z 525 and m/z 541 contain peaks at m/z 134 indicating that the phenyl ring is not the site of presumably what represents hydroxylation. The shift in mass of the y_2''

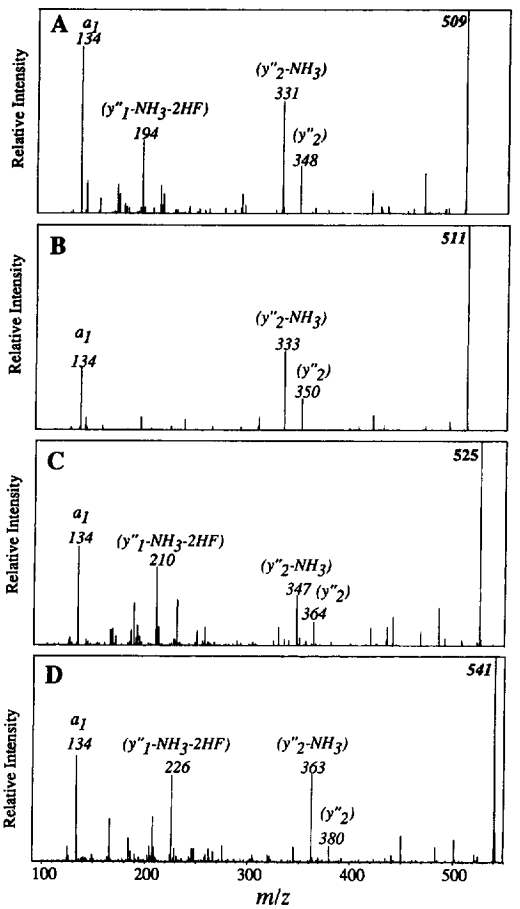

Fig. 7. Tandem mass spectra of protonated analytes detected in bile: (A) parent compound, m/z 509; (B) m/z 511; (C) m/z 525; (D) m/z 541.

and (y''_2-NH_3) ions by 16 and 32 u, respectively, for CID product ions of m/z 525 and 541 indicates that the biotransformation occurs on either the proline ring or arginine portion of the tripeptide, not on the Phe. The key diagnostic ions to further establish structural information arise at m/z 210 (product of m/z 525) and m/z 226 (product of m/z 541). These mass spectral peaks are consistent with the (y_1''-NH_3-2HF) ions for which m/z 194 is detected in the tandem mass spectrum of protonated I. These data indicates the sites of biotransformation are on the arginine side chain or the aliphatic chain extended from the fluoroalkyl moiety of the molecule.

In addition, upon LC–MS analysis of I, a minor peak was present in the mass spectrum which was

consistent with the structure representing the addition of water (data not shown). This hydration occurred during the ionization process, likely at C5. It was of interest to note that this hydration was not evident upon examination of the corresponding reconstructed ion chromatograms in the LC–MS analysis for the metabolites detected with M_r 524 and 540. Given the MS–MS data which confine the oxidation to the C-terminal region of the molecule, we propose that this observation regarding lack of hydration in the ionization process may be accounted for if oxidation occurred at C1 or C2. If hydroxylation is at either of these two sites, upon ESI ionization intra-molecular hydration at C5 may occur forming a stable 5- or 6-membered ring, thereby precluding hydration by a water molecule. Although the mass spectral data do not unequivically enable identification of these metabolites, the data clearly eliminate some of the possible sites as locations of the biotransformation.

4. Conclusion

A system consisting of narrow-bore HPLC chromatography with simultaneous detection by radioactivity monitoring and tandem mass spectrometry was characterized with respect to maintenance of chromatographic integrity and detection limits. The HPLC effluent was split and a post-column make-up flow was added to flow directed towards the radioactivity detector containing a solid glass cell. For compound I, the presence of TFA in the make-up solvent ensures good chromatographic peak shape in the ^{14}C profile, presumably because adverse silanol reactions are impeded. Sensitivity was demonstrated in the analysis of radiolabeled sample with 1100 dpm. Two peaks, representing the diastereomers (550 dpm per isomer), were detected each with a S/N of 3.

There are a number of potential applications for this system. This system may be useful in characterizing radioactive standards, used for example, in dosing solutions. Not only could ^{14}C purity be assessed but structural information is provided concurrently. This system may also be used in characterization of drug metabolites generated from radiolabeled drug in both in vivo and in vitro metabolism studies. Metabolites may be rapidly located via the ^{14}C detection, while structural information can be obtained by mass spectrometry. The on-line radioactivity monitoring ensures that no major metabolites are missed by tandem mass spectrometry screening which is designed to selectively detect drug related compounds. Conversely, the sensitivity offered by the mass spectrometry detection may discern minor metabolites not recognized by the radioactivity monitor. We used the system to rapidly characterize biliary metabolites of I. This study serves to demonstrate the possible limitation of relying solely on mass spectrometry for assigning chemical structures to metabolites as complete structural characterization of all metabolites was not possible. However, the procedure did not require sample processing and all of the structural information was provided in the HPLC analysis. If the metabolites were isolated by fraction collection and then analyzed, additional spectroscopic characterization could be performed, yet no additional structural information could be offered by mass spectrometry. Techniques such as that described here as well as hyphenated HPLC–NMR techniques [15] which can rapidly provide structural information on metabolites in biological matrices are useful tools which aid in the expeditious progression of drug development, particularly in early stage drug discovery support studies.

Acknowledgments

We would like to thank Paul Brown, Drs. John Ho, John Ling, Paul Toren and Richard Thompson for helpful discussions and comments during the preparation of this manuscript.

References

[1] R.J. Perchalski, R.A. Yost and B.J. Wilder, Anal. Chem. 54 (1982) 1466.
[2] R.A. Yost, R.J. Perchalski, H.O. Brotherton, J.V. Johnson and M.B. Budd, Talanta, 31 (1984) 929.
[3] M.S. Lee and R.A. Yost, Biomed. Environ. Mass Spectrom., 15 (1988) 193.
[4] P. Rudewicz and K.M. Straub, Anal. Chem., 58 (1986) 2928.
[5] T.R. Covey, E.D. Lee and J.D. Henion, Anal. Chem., 58 (1986) 2453.

[6] J.E. Coutant, R.J. Barbuch, D.K. Satonin and R.J. Cregge, Biomed. Environ. Mass Spectrom., 14 (1987) 325.
[7] D. Thamassen, P.G. Pearson, J.T. Slattery and S.D. Nelson, Drug Metab. Dispos., 19 (1991) 997.
[8] T. Kondo, K. Yoshida and S. Tanayama, Biol. Mass Spectrom., 23 (1994) 323.
[9] J.J. Vrbanac, I.A. O'Leary and L. Baczynskyj, Biol. Mass Spectrom., 21 (1992) 517.
[10] D.A. Whitman, v. Abbot, K. Fregien and L.D. Bowers, Ther. Drug Monit., 15 (1993) 552.
[11] C. Fenselau and P.B.W. Smith, Xenobiotica, 22 (1992) 1207.
[12] S. Naylor, M. Kajbaf, J.H. Lamb, M. Jahanshahi and J.W. Gorrod, Biol. Mass Spectrom., 22 (1993) 388.
[13] P.J. Jackson, R.D. Brownsill, A.R. Taylor and B. Walther, J. Mass Spectrom., 30 (1995) 446.
[14] L.C.E. Taylor, R. Singh, S.Y. Chang, R.L. Johnson and J. Schwartz, Rapid Commun. Mass Spectrom., 9 (1995) 902.
[15] A.E. Mutlib, J.T. Strupczewski and S.M. Chesson, Drug Metab. Dispos., 23 (1995) 951.
[16] E. Gelpi, J. Chromatogr. A., 703 (1995) 59.
[17] R.P. Schneider, K.M. Davis, P.B Inskeep and H.G. Fouda, Proceedings of the 42nd ASMS Conference on Mass Spectrometry and Allied Topics, Chicago, IL, 1994.
[18] G.A. Schultz and J.N. Alexander, Proceedings of the 44th ASMS Conference on Mass Spectrometry and Allied Topics, Portland, OR, 1996.
[19] A.C. Veltkamp, J. Chromatogr., 531 (1990) 101.
[20] P. Roepstorff and J. Fohlman, Biomed Mass Spectrom., 11 (1984) 601.
[21] K. Biemann, Biomed Mass Spectrom., 16 (1988) 99.
[22] R.P. Grese, R.L. Cerny and M.L. Gross, J. Am. Chem. Soc., 111 (1989) 2835.
[23] J. Hauptmann, B. Kaiser, M. Paintz and F. Markwardt, Biomed. Biochim. Acta, 46 (1987) 445.
[24] K. Oda, K. Ohtsu, Y. Tamao, R. Kikumoto, A. Hijikata, K. Kinjo and S. Okamoto, Kobe J. Med Sci., 26 (1980) 11.
[25] J. Hauptmann and B. Kaiser, Pharmazie, 46 (1991) 57.